New instability windows for rotating neutron stars

M.E. Gusakov, A.I. Chugunov, E.M. Kantor
Ioffe Institute, Saint-Petersburg

We reanalyze the r-mode instability in rotating superfluid neutron stars. To this aim we develop a model of resonance interaction of normal $m = 2$ r-mode with superfluid modes. We show that this interaction dramatically modifies the instability window, that is the region of stellar spin frequencies and temperatures in which a neutron star becomes unstable with respect to radiation of gravitational waves. This modification allows us to formulate an evolution scenario for neutron stars in LMXBs that can explain all rapidly rotating neutron stars observed in LMXBs, as well as the existence of millisecond pulsars (see **arXiv:1305.3825** and the presentation 'Observationally consistent evolution scenario for neutron stars in LMXBs' by Gusakov, Chugunov, and Kantor for more details).

I. INTRODUCTION

Neutron stars (NSs) are compact *rotating* objects with the mass $M \sim 1.4\,M_\odot$ and radius $R \sim 10$ km (see, e.g., [1]; $M_\odot$ is the solar mass). Rotation leads to the appearance of the so-called *inertial* oscillation modes in NSs, whose restoring force is the Coriolis force [2]. A particular, but the most interesting class of inertial modes is *r-modes.* These modes, neglecting dissipation, are subject to gravitational-driven instability at *any* NS spin frequency ν [3]. An account for dissipation reduces the instability window, that is the region of spin frequencies ν and red-shifted internal temperatures T^∞, in which an NS is unstable with respect to emission of gravitational waves.

Observations of NSs in low-mass X-ray binaries (LMXBs) allow to measure ν and estimate T^∞ for some objects (see, e.g., [4–6] and Fig. 1). It turns out that many of the rapidly rotating warm sources fall well outside the stability region, that makes their interpretation problematic [4–6].

This work is devoted to a possible resolution of that problem. Our key idea consists in that to study evolution of NSs in LMXBs one has to correctly take into account the resonance interaction between the normal oscillation $m = 2$ r-mode and superfluid inertial modes, which occurs at some fixed values of T^∞ (see Sec. III). Such resonance interaction has been completely ignored in the literature so far.

II. "STANDARD" INSTABILITY WINDOWS AND OBSERVATIONAL DATA

All calculations here are carried out for a canonical NS with the mass $M = 1.4M_\odot$ and radius $R = 10$ km, whose core is composed of neutrons (n), protons (p), and electrons (e). Theoretical calculations predict that at $T \lesssim 10^8 \div 10^{10}$ K nucleons in the internal layers of NSs are in superfluid state. This is confirmed by observations of cooling isolated NSs [7, 8].

In superfluid NSs two types of inertial modes can exist, *normal* and *superfluid* [9–11]. Normal modes (i^o-modes) describe co-moving oscillations of superfluid and normal matter components and are similar to the corresponding modes of a nonsuperfluid star [11–13]. The superfluid modes correspond to counter-moving oscillations and are absent in normal stars. Generally these two types of modes are decoupled and almost do not interact. Among i^o-modes we only consider the normal r-modes (r^o-modes) with $m = 2$ and $m = 3$, since they are the most unstable ones [14]. Their gravitational radiation timescale is $\tau_{\rm GR} \approx \tau_{\rm GR\,0}(\nu/1\,{\rm kHz})^{-2\,m-2}$ [14, 15] (where $\tau_{\rm GR\,0} \approx -46.4$ s and -1250 s for $l = m = 2$ and $l = m = 3$ r^o-modes, respectively).

Dissipation acts to suppress the instability; the corresponding timescale will be denoted as $\tau_{\rm Diss}$. For i^s-modes the main dissipation mechanism is *mutual friction* [9, 10]. It tends to equalize the velocities of normal and superfluid components. Hence, for i^s-modes $\tau_{\rm Diss} = \tau_{\rm MF} \approx \tau_{\rm MF\,0}\,\frac{\Omega_0}{\Omega}$, where $\tau_{\rm MF\,0} \approx 2.5$ s, $\Omega_0 \equiv \sqrt{3\,G\,M/(4R^3)} \approx 1.180\times10^4\,{\rm s}^{-1}$, $\Omega = 2\pi\nu$. In contrast, for r^o-modes the mutual friction dissipation can be neglected since the normal and superfluid components are comoving for these modes. Thus, we consider dissipation due to the shear viscosity as our *minimal* model for damping of r^o-modes. In that case $\tau_{\rm Diss} = \tau_{\rm S} \approx \tau_{\rm S\,0}\,(T_8^\infty)^2$, where $T_8^\infty \equiv T^\infty/(10^8\,{\rm K})$; $\tau_{\rm S\,0} \approx 2.2\times10^5$ s for $l = m = 2$ r^o-mode and $\tau_{\rm S\,0} \approx 2.4\times10^4$ s for $l = m = 3$ r^o-mode. It is crucial that damping of i^s-modes is much more efficient than that of r^o-modes.

The condition $1/\tau_{\rm GR} + 1/\tau_{\rm Diss} < 0$ determines the instability window. Dashed line in Fig. 1 shows its boundary ("the instability curve") for $m = 2$ r^o-mode. The stability region for $m = 2$ r^o-mode is filled with grey. Also shown are the spin frequencies ν and internal red-shifted temperatures T_8^∞ of 20 NSs in LMXBs, whose parameters can be deduced from observations. One can see that many sources in Fig. 1 lies outside the stability region, where the probability to observe them is negligibly small. All available in the literature explanations of this fact (see, e.g., [4–6])

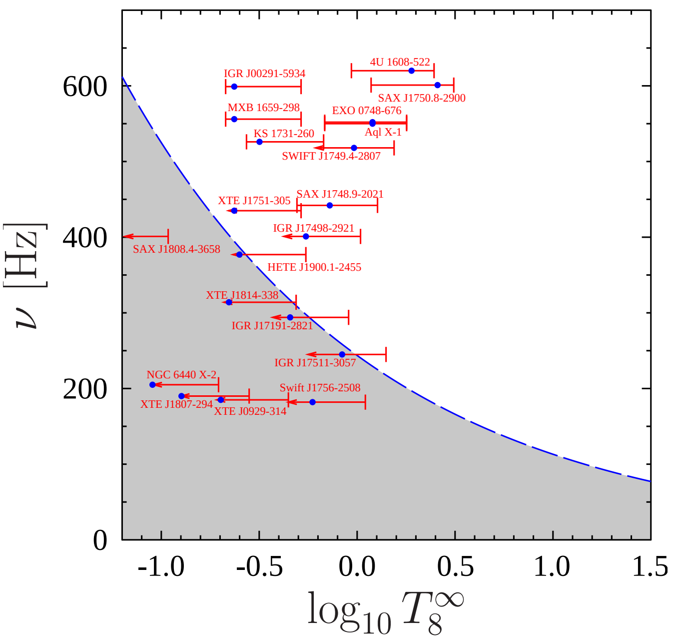

FIG. 1: Spin frequency vs internal redshifted temperature for NSs in LMXBs. The frequencies and temperatures of 20 sources are shown by small filled circles. Error bars describe uncertainties in T^∞ related to poorly constrained envelope composition. The "standard" stability region for r^o-mode with $m = 2$ is filled with grey, its boundary is shown by dashed line.

invoke rather artificial assumptions that either cannot be fully justified or even contradict the up-to-date calculations available in the literature.

III. RESONANCE INTERACTION OF SUPERFLUID AND NORMAL MODES

While the eigenfrequencies ω of r^o-modes are temperature independent, those of i^s-modes depend on temperature. Thus, at some temperature the eigenfrequencies of i^s- and r^o-modes can approach one another and start to interact resonantly. As a result of such interaction, the superfluid i^s-mode transforms into the normal r^o-mode and vice versa; that is, an avoided crossing of modes is formed in the $\omega - T^\infty$ plane. In Fig. 2(a) we (schematically) present oscillation frequency ω as a function of T^∞ for two neighboring modes of a superfluid NS, experiencing an avoided crossing at $T^\infty = T_0^\infty$. At $T^\infty < T_0^\infty$ the role of the r^o-mode is played by the mode II, while the mode I behaves as the superfluid i^s-mode. The resonance interaction of the modes I and II significantly affects their dissipation timescales $\tau_{\rm Diss}$, as it is illustrated in Fig. 2(b,c).

Such a behavior of oscillation modes was confirmed by the analysis of oscillations of superfluid nonrotating NSs [13, 16, 17]. Inertial modes (in particular, r^o-modes) in rotating NSs should behave in a similar way. The results of Refs.[9, 10, 18, 19] confirm this statement. This allows us to formulate the main assumption of our model: *An oscillation mode of a superfluid rotating NS, which behaves, at some T^∞, as a normal quadrupole $m = 2$ r-mode (r^o-mode) can, as the temperature gradually changes, transform into a superfluid-like inertial mode (i^s-mode).*

Let us qualitatively describe such resonant transformation of the modes. As we mentioned above, far from the avoided crossings the superfluid and normal modes almost do not interact (their interaction is parameterized by the small *coupling parameter* $s \sim 0.0001 \div 0.05$). Assume, that the eigenfunction of a superfluid mode is $\Psi_{\rm sfl}$ and the eigenfunction of a normal mode is $\Psi_{\rm norm}$. In the vicinity of an avoided crossing the modes start to interact resonantly so that the eigenfunctions of the exact solution should be presented as a linear superposition of $\Psi_{\rm norm}$ and $\Psi_{\rm sfl}$. In particular, in Fig. 2 an avoided crossing occurs between the modes I and II. Denoting the corresponding eigenfunctions as $\Psi_{\rm I}$ and $\Psi_{\rm II}$, one can write

$$\Psi_{\rm I} = -\sin\theta(x)\, \Psi_{\rm norm} + \cos\theta(x)\, \Psi_{\rm sfl}, \tag{1}$$
$$\Psi_{\rm II} = \cos\theta(x)\, \Psi_{\rm norm} + \sin\theta(x)\, \Psi_{\rm sfl}, \tag{2}$$

where the function $\theta(x)$ determines how the normal mode transforms into superfluid one (and vice versa). This function depends on the parameter $x \equiv (T^\infty - T_0^\infty)/\Delta T^\infty$ [see Fig. 2(a)] and ranges from 0 to $\pi/2$ on a temperature

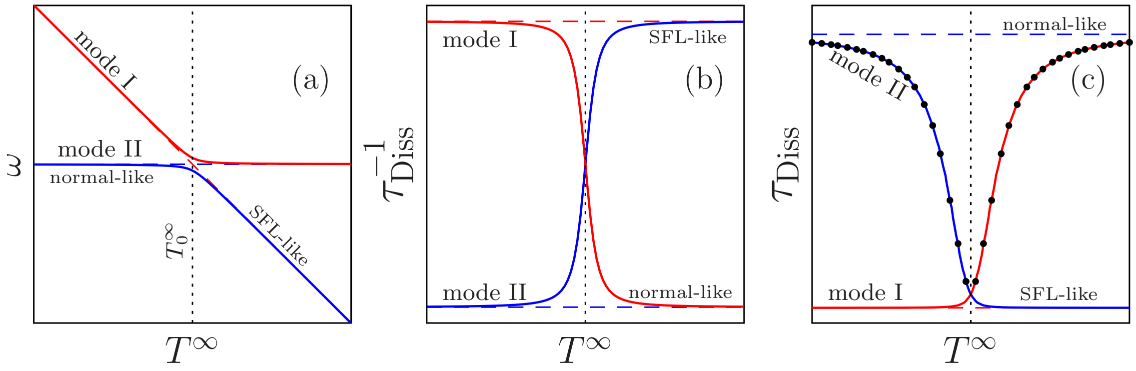

FIG. 2: A schematic plot showing oscillation frequencies ω for a superfluid NS (a), inverse damping timescale $\tau_{\rm Diss}^{-1}$ (b), and $\tau_{\rm Diss}$ (c) versus temperature T^∞ for two oscillation modes (I and II), experiencing avoided crossing at $T^\infty = T_0^\infty$. Dashes correspond to an approximation of independent oscillation modes ($s = 0$), solid lines are plotted for exact solution allowing for the interaction of modes I and II. Vertical dotted line indicates T_0^∞. Filled circles in panel (c) illustrate the results shown in figure 12 of Ref. [9].

scale specified by the characteristic width ΔT^∞ of the avoided crossing, $\Delta T^\infty \sim s\, T_0^\infty$. The exact form of the function $\theta(x)$ can be found only by direct solution to the coupled oscillation equations. However, using as the analogy the problem of intersection of electron terms in molecules (see, e.g., Ref. [20], §79), one can immediately write down an approximate expression for $\theta(x)$ that correctly reproduces its main properties,

$$\theta(x) = \frac{1}{2}\left[\frac{\pi}{2} + \mathrm{arctg}(x)\right]. \tag{3}$$

Consider, for example, the mode II. At $x \to -\infty$ one has $\theta(x) \to 0$, and it follows from Eq. (2) that the mode II is in normal-like regime ($\Psi_{\rm II} = \Psi_{\rm norm}$); at $x \to +\infty$ one obtains $\theta(x) \to \pi/2$, which corresponds to superfluid-like behavior of the mode II ($\Psi_{\rm II} = \Psi_{\rm sfl}$).

Using Eqs. (1)-(3) one can calculate the damping timescales for the mode I and II. In particular, for the mode I one has

$$\frac{1}{\tau_{\rm X}} \approx \frac{1}{\tau_{\rm X}^{\rm norm}} \sin^2\theta(x) + \frac{1}{\tau_{\rm X}^{\rm sfl}} \cos^2\theta(x) \tag{4}$$

and for the mode II

$$\frac{1}{\tau_{\rm X}} \approx \frac{1}{\tau_{\rm X}^{\rm norm}} \cos^2\theta(x) + \frac{1}{\tau_{\rm X}^{\rm sfl}} \sin^2\theta(x). \tag{5}$$

These are the main formulas of our approximate model. Their use for X = S, MF, GR (shear viscosity, mutual friction, and gravitational radiation) enables us to plot the instability windows for the real oscillation modes (similar to the modes I and II shown in Fig. 2).

IV. REALISTIC INSTABILITY WINDOWS

Instability curves for the modes I (solid red line) and II (solid blue line) are shown in Fig. 3(a,b). At low T^∞ the mode II behave as r^o-mode, while the mode I – as i^s-mode (as in Fig. 2). The curves are obtained by making use of Eqs. (4)–(5) with the coupling parameter $s = 0.001$. The panel (b) is a version of panel (a), but plotted in a different scale. The dotted line in Fig. 3(a,b) corresponds to the temperature $T_0^\infty = 1.5 \times 10^8$ K, at which the modes I and II experience avoided crossing. In addition, Fig. 3(a,b) shows the instability curves for: (*i*) octupole $m = 3$ r^o-mode (grey solid line); (*ii*) $m = 2$ r^o-mode (blue dashed line); (*iii*) superfluid i^s-mode with $m = 2$ (red dashed line). The latter curves (*i*)–(*iii*) are obtained using the approximation $s = 0$ (neglecting the interaction between the superfluid and normal modes).

As one would expect, far from the avoided crossing point the solid (modes I and II) and dashed (r^o and i^s-modes) lines almost coincide. The region, where $m = 2$ modes I, II, and the octupole $m = 3$ r^o-mode are simultaneously stable, is filled with grey in Fig. 3(a,b). The presence of the 'stability peak' at $T^\infty \approx T_0^\infty$ is an important characteristic

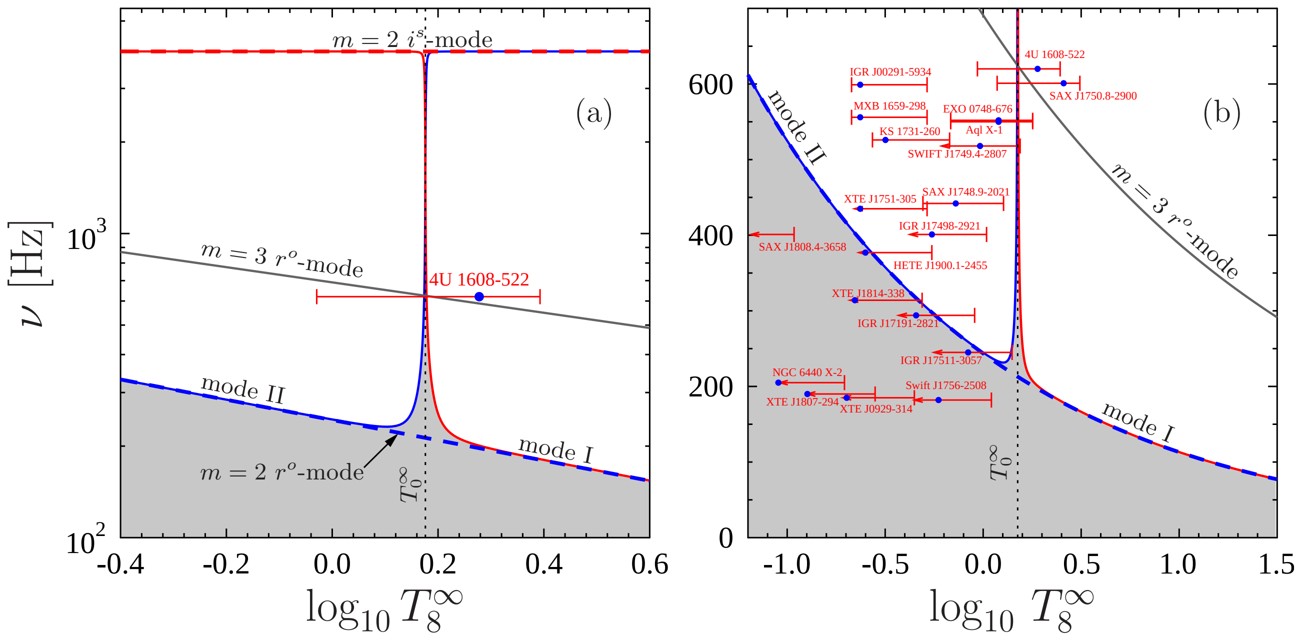

FIG. 3: Instability curves for superfluid NS oscillations. The red and blue solid curves correspond to $m = 2$ modes I and II, which experience avoided crossing at $T_0^\infty = 1.5 \times 10^8$ K. Coupling parameter was chosen to be $s = 0.001$. The dashed red and blue curves correspond to $m = 2$ r^o- and i^s-mode plotted under assumption that they are completely decoupled ($s = 0$). The grey line is the instability curve for $m = 3$ r^o-mode, plotted ignoring the resonance coupling with the superfluid modes. The temperature T_0^∞ is shown by the vertical dotted line. The panel (b) shows temperatures and frequencies of the observed sources. Only the fastest source 4U 1608-522 is shown in the panel (a).

feature of this region. The height of the peak is determined by the lowest-frequency intersection of the mode II instability curve with the other instability curves. The instability curves for the modes I and II intersect at a very high frequency $\nu \approx 1580$ Hz; hence, the lowest-frequency intersection corresponds to that with the octupole $m = 3$ r^o-mode and occurs at $\nu \approx 625$ Hz. As a result, at $T^\infty = T_0^\infty$ the most unstable mode is $m = 3$ r^o-mode, and the height of the stability peak is $\nu \approx 625$ Hz.

It can be shown that, in the course of its evolution, any NS with equilibrium temperature less than T_0^∞ will spend substantial fraction of time climbing up the left side of the stability peak. This naturally explains the high spin frequencies of the sources 4U 1608-522, SAX J1750.8-2900, EXO 0748-676, Aql X-1, and SWIFT J1749.4-2807, which can be interpreted as moving along the peak in Fig. 3(b).

In reality, the normal $m = 2$ r-mode mode can experience more than one avoided crossing with the superfluid modes. To illustrate this idea, we demonstrate in Fig. 4 the instability curves in case of two avoided crossings of oscillation modes. The first avoided crossing takes place at $T^\infty = 4.5 \times 10^7$ K between the mode III (the violet solid line), which behaves as $m = 2$ r^o-mode at low T^∞, and the mode II (the blue solid line). For this avoided crossing the coupling parameter was chosen to be $s = 0.01$. The second avoided crossing of modes I and II is discussed above and takes place at $T^\infty = 1.5 \times 10^8$ K. In this case the mode II behaves as $m = 2$ r^o-mode only at intermediate temperatures 6×10^7 K $\lesssim T^\infty \lesssim 1.3 \times 10^8$ K. At higher and at lower temperatures it transforms into superfluid modes, which are different. It is easy to demonstrate that, for low enough $T_{\rm eq}^\infty \lesssim 4 \times 10^7$ K, the evolution track goes along the left (low-temperature) boundary of the first stability peak, corresponding to the avoided crossing of the modes II and III (i.e., along the violet line in Fig. 4). One sees that two avoided crossings are already sufficient to explain *all* the existing observations of frequencies and quiescent temperatures of NSs in LMXBs.

V. CONCLUSIONS

We show that instability windows of rotating NSs are significantly modified by accounting for the resonance interaction of normal oscillation $m = 2$ r-mode (r^o-mode) and superfluid inertial modes (i^s-modes). In the vicinity of a resonance the eigenfunctions of i^s-mode become admixed with the eigenfunctions of $m = 2$ r^o-mode which results in

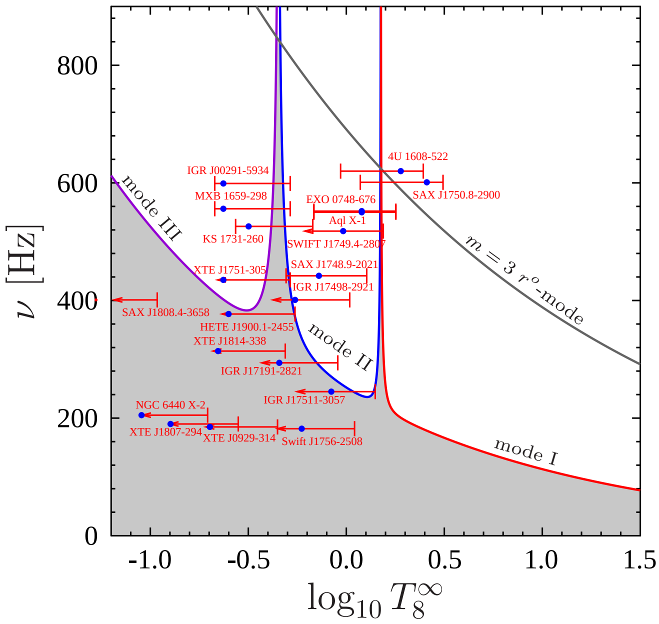

FIG. 4: An example of the stability curves in case of two avoided crossings of $m = 2$ oscillation modes of a superfluid NS. As in Fig. 3, the solid red and blue lines are plotted for the modes I and II experiencing an avoided crossing at $T^\infty = 1.5 \times 10^8$ K (the coupling parameter $s = 0.001$). An additional violet solid line corresponds to the mode III, which exhibit an avoided crossing with the mode II at $T^\infty = 4.5 \times 10^7$ K. This avoided crossing is drawn for $s = 0.01$. Other notations are the same as in Fig. 3.

the enhanced damping of r^o-mode due to the mutual friction dissipation. In the $\nu - T^\infty$ plane, this effect is manifested by the appearance of sharp 'stability peaks' over the standard (usually considered) stability region of fast rotating NSs (Figs. 3 and 4; the stability region is filled with grey there). An analysis of evolution of NSs in LMXBs taking into account the stability peaks shows that the stars spend significant amount of time climbing the left sides of these peaks in the region, which has been previously thought to be unstable with respect to excitation of r-modes. As a consequence, the real limit on the spin frequency of NSs is set by the instability curve for the octupole $m = 3$ r^o-mode. This result allows us to naturally explain the rapidly rotating warm NSs in LMXBs within the minimal assumptions about the properties of superdense matter (see Fig. 4). Moreover, this result agrees with the predicted [21, 22] abrupt cut-off above ~ 730 Hz of the spin frequency distribution of accreting millisecond X-ray pulsars.

[1] P. Haensel, A. Y. Potekhin, and D. G. Yakovlev, *Neutron Stars 1 : Equation of State and Structure* (2007).
[2] W. Unno, Y. Osaki, H. Ando, H. Saio, and H. Shibahashi, *Nonradial oscillations of stars* (1989).
[3] N. Andersson, ApJ **502**, 708 (1998), arXiv:gr-qc/9706075.
[4] W. C. G. Ho, N. Andersson, and B. Haskell, Physical Review Letters **107**, 101101 (2011), 1107.5064.
[5] B. Haskell, N. Degenaar, and W. C. G. Ho, MNRAS **424**, 93 (2012), 1201.2101.
[6] S. Mahmoodifar and T. Strohmayer, ArXiv e-prints (2013), 1302.1204.
[7] M. E. Gusakov, A. D. Kaminker, D. G. Yakovlev, and O. Y. Gnedin, MNRAS **363**, 555 (2005), arXiv:astro-ph/0507560.
[8] P. S. Shternin, D. G. Yakovlev, C. O. Heinke, W. C. G. Ho, and D. J. Patnaude, Mon. Not. R. Astron. Soc. **412**, L108 (2011).
[9] U. Lee and S. Yoshida, ApJ **586**, 403 (2003), arXiv:astro-ph/0211580.
[10] S. Yoshida and U. Lee, MNRAS **344**, 207 (2003), arXiv:astro-ph/0302313.
[11] E. M. Kantor and M. E. Gusakov, in *Electromagnetic Radiation from Pulsars and Magnetars*, edited by W. Lewandowski, O. Maron, and J. Kijak (2013), vol. 466 of *Astronomical Society of the Pacific Conference Series*, p. 211.
[12] M. E. Gusakov and E. M. Kantor, Phys. Rev. D **83**, 081304 (2011), 1007.2752.
[13] M. E. Gusakov, E. M. Kantor, A. I. Chugunov, and L. Gualtieri, MNRAS **428**, 1518 (2013), 1211.2452.
[14] N. Andersson and K. D. Kokkotas, International Journal of Modern Physics D **10**, 381 (2001), arXiv:gr-qc/0010102.
[15] L. Lindblom, B. J. Owen, and S. M. Morsink, Physical Review Letters **80**, 4843 (1998), arXiv:gr-qc/9803053.
[16] E. M. Kantor and M. E. Gusakov, Phys. Rev. D **83**, 103008 (2011), 1105.4040.
[17] A. I. Chugunov and M. E. Gusakov, MNRAS **418**, L54 (2011), 1107.4242.

[18] L. Lindblom and G. Mendell, Phys. Rev. D **61**, 104003 (2000), arXiv:gr-qc/9909084.
[19] S. Yoshida and U. Lee, Phys. Rev. D **67**, 124019 (2003), arXiv:gr-qc/0304073.
[20] L. Landau and E. Lifshits, *Quantum Mechanics: Non-Relativistic Theory* (Butterworth-Heinemann Limited, 1977), ISBN 9780750635394, URL `http://books.google.ru/books?id=J9ui6KwC4mMC`.
[21] D. Chakrabarty, E. H. Morgan, M. P. Muno, D. K. Galloway, R. Wijnands, M. van der Klis, and C. B. Markwardt, Nature **424**, 42 (2003), arXiv:astro-ph/0307029.
[22] D. Chakrabarty, in *American Institute of Physics Conference Series*, edited by R. Wijnands, D. Altamirano, P. Soleri, N. Degenaar, N. Rea, P. Casella, A. Patruno, and M. Linares (2008), vol. 1068 of *American Institute of Physics Conference Series*, pp. 67–74, 0809.4031.